Since January 2020 Elsevier has created a COVID-19 resource centre with free information in English and Mandarin on the novel coronavirus COVID-19. The COVID-19 resource centre is hosted on Elsevier Connect, the company's public news and information website.

Journal of Photochemistry and Photobiology 10 (2022) 100108

Contents lists available at ScienceDirect

Journal of Photochemistry and Photobiology

journal homepage: www.sciencedirect.com/journal/journal-of-photochemistry-and-photobiology

Latitude impact on pandemic Sars-Cov-2 2020 outbreaks and possible utility of UV indexes in predictions of regional daily infections and deaths

Helena Nandin de Carvalho *

Independent, Pç José Fontana 12- 3, 1050-129 Lisbon, Portugal

ARTICLE INFO

Keywords:
Pandemic Covid-19
Solar UV
UV indexes
Latitude
UV-induced immunosuppression
Satellite

ABSTRACT

The importance of two related factors - latitude and solar ultraviolet radiation - has been insufficiently recognized as determining the spread of pandemic Sars-CoV-2 outbreaks across the globe. In this study we provide evidence of the impact of latitude and investigate how daily RT-PCR diagnosed infections and deaths are quantitively correlated with the UV component of solar light. Here, we present regression analyses using daily national numbers from Austria and from Portugal with daily ultraviolet indexes of two selected locations in these territories, obtained from a satellite source. These countries, have similar surfaces areas and population size but Austria's mean latitude is 9° up-north. The equations derived from regression analyses of those two variables are comparable for both countries, fit best the fall (2nd) pandemic wave and can be a useful non-R(t) (ratio of transmission at a particular time) dependent predictive tool. Similar equations were derived for deaths that follow infections within a few weeks delay. Strong correlations depend on the size of the region/country from which infections are collected, the robustness of screening practices, ideally kept through weekends and holidays. Besides the forecasting usefulness of such correlations, these findings also suggest that covid-19 transmission co-exists with a Sars-Cov-2 specific UV-induced immunosuppression response. While in 2020, intensity of pandemic spring and fall waves reflect a solar UV-light modulation, we relate exceptional low temperature and humidity with additional waves, as the winter 2020/2021 3rd wave, felt in the western European countries. This work may help understanding this Pandemic phenomenon and dealing with similar catastrophes in the future.

1. Introduction

In earlier 2020, the World was stricken by a rapid spread of a mild to severe infectious disease unseen, in its extent and gravity, since the so-called Spanish Flu or pneumonia which affected the planet in 1918 and 1919 [1,2]. The first outbreak of this acute respiratory syndrome occurred in late 2019 in China, caused by a new virus SARS-CoV-2 [3] of uncertain origin.

Despite today's increased testing capacity, better symptomatic care, as the use of ventilators and access to drugs, general public health strategies to protect populations [4] are basically the same of the pandemic diseases of the past century. They range from simpler hygiene practices to recommended or imposed restrictive behaviors, including disruptive lockdowns which brought misery and led to devastating economic distress across the world.

As herd immunization through infection seemed unlikely, governance set pressure on Pharmaceutical Industry who, faster than never before, provided a variety of vaccines. This undeniable breakthrough which is expected to drop the mortality of the disease, did not come in time to avoid the over 4 million of Covid-19 deaths at the date of this article, not counting the non-Covid19 excess mortality registered in many countries.

While so much science has been devoted to prevention and treatment of infections by Sars-CoV-2, there is still room for the development of tools that can help mastering similar pandemic crisis in the future. Improving predictability of such phenomena appears a useful objective that may facilitate allocation of adequate human and financial resources and help remediation of the economic impact.

Epidemiological models to forecast the progression of the number of infections are complex, based on persons interactions and social [5] behaviors. Most predictions failed on the earlier onset of a 2nd wave [6], and on its amplitude, 10 to 15 times that of the 1st wave in European countries, despite enforcement of masks in most of them and of the drastic reduction of tourism. While nothing is wrong about mathematical models [7] the problem lies on current pandemics which is far from being completely understood.

* Corresponding author.
E-mail address: Helena.nandin@hotmail.com.

https://doi.org/10.1016/j.jpap.2022.100108

Available online 13 January 2022

Following the pandemic's evolution from its early onset, we were intrigued, as possibly many others, by the fact that the epicenter of the infection was "travelling" from east to west, soon brought to center of Europe with limited spread in those countries in the south of China. In Europe, Lombardy, province in the north of Italy (lat. approx. 45° 40′N), suffered a severe outbreak, while the south was not so badly affected and neither were southern Mediterranean regions of Greece and Portugal, such as the Algarve, or Northern Africa.

We also observed from our standpoint in Lisbon, where the first cases were detected in earlier March that bright sunny days tended to deliver fewer positive tests of Covid-19 infection than those of instability and heavy cloudy sky. Looking for several days at the world weather forecasts, this same trend was observed in countries or regions with prolonged instability and depression conditions.

This led to the hypothesis of involvement of an electromagnetic component of the sunlight, particularly the ultraviolet radiation, known to participate in nature common daily events, promoting sometimes beneficial, sometimes harmful effects.

To the best of our knowledge this is one of the first studies quantitatively correlating daily reported cases of Covid-19 with a measurable daily unit derived from the UV solar radiation, mainly in the UVB region, and exploring the potential of this relation as an alternative forecasting tool of the new cases and fatalities.

The ultraviolet index (UVI) was developed as an indicator serving as guidance to the general public on the health risks derived from sun exposition and relevant to the UV-induced erythema [8]. The calculation the UV indexes requires an equation multiplying a constant by the integration of a range of wavelengths where this biological effect is measurable [9], the respective solar spectral irradiance component at the surface expressed in W/m^2nm-1 and the distance to the sun at each location. UV irradiation depends on the solar elevation, changing with latitude, season and time of the day. Other parameters and events affecting the radiation felt at ground level introduce uncertainty in the forecast of indexes. The relevance of some earth's surface morphology as altitude, soil reflection (particularly by presence of snow) along with atmosphere variables such as presence of clouds, tropospheric ozone profile, total ozone and aerosol properties, were discussed by Allaart. M. et al. (2004) when deriving an empirical model to predict UV indexes [10] (UVI). This model fitted UV indexes values to Total Ozone measurements and Solar Zenith Angles (SZA) making them applicable at a wider range of SZA (0 to 90°) and useful to calculate globally those indexes in a cloud free sky. Atmospheric pollution arising from industrial or human activity is not considered in the indexes calculated. However, events like clouds, rain, can reduce these indexes and correction factors may then apply.

The relevance of these UV indexes for this study is that they ponder the effect of geographic location and amount of radiation received throughout the year. As directly related to latitude, they decrease from the equator to the north and south polos.

Change in meteorological conditions is for long modulating the established seasonality characterizing several respiratory infectious outbreaks in different regions of the globe.

Previous work by Ianevski et al. (2019) [11] found that low temperature and UV radiation were the most predictive of six factors for retaining high infectivity of the Influenza subtypes affecting six Scandinavian and northern Baltic countries in 2017 and 2018.

Other studies, reporting the effect mainly of temperature and humidity in the variability of incidence of Sars-Cov-2 across regions or countries, became available after this research was in progress and were useful in supporting interpretation of observations reported further in this article.

2. Materials and methods

Raw data, (i.e. not smoothed by any kind of ratio regarding population), was collected from the database "our world in data" [12], and up-to-dated periodically to integrate eventual corrections by primary sources. The data extracted for countries addressed in this study consisted in numbers of daily positive cases, daily deaths and daily tests, population, population density and median age of population. The source of UV indexes and respective cloud modifying factors, when applied, is the *Temis v2.0 UV index and UV dose overpass file* [13] of the Temis (Tropospheric Emission Monitoring Internet System) satellite database, that monitors the ozone layer in the troposphere. The values extracted are those of the clear sky index reported daily for Vienna (long. 16.35°W and lat. 48.23°N) and for Lisbon (long.−9.15° lat. 38.77° N), found in the 1st column of the 16 columns of respective grids. These clear sky daily indexes are reproduced in the suplementary material 2 Tables S2-a and b along with those of Berlin, Paris, Ispra and London while they are increasing, at the occasion of the 1st wave and when they are decreasing, up to the end of the 2nd wave. For more details see supplementary material 1.

3. Results

3.1. Analysis of latitude as a determinant factor in the severity of the 2020 Sars-Cov-2 outbreaks

In an unpublished study looking at the impact of latitude on this pandemic crisis, we compared groups of countries with borders within a fixed range of parallels, and their respective records of cumulative Covid-19 confirmed cases and deaths at two reference dates, 6 months apart. Despite difficulties in eliminating the effect of other characteristics such as population density and median age, it became clear that countries between parallels 31° N and 60° N were the most severely affected. An example, covering this corridor is summarized in Fig. 1, which compares diagnosed cases reported on August 28, 2020 in four well developed countries at different latitudes, three of them (South Korea, Italy and Great Britain) with similar population size. Located at lower latitude, South Korea, (51.2 million of inhabitants), registered 19 400 positive cases (0.38‰) and 321 deaths (not shown), while Netherlands located at higher latitude, with one third of the population (approximately 17.1 million), but comparable density (508.54 versus 527.97 inhab./km^2 in the Asiatic country) had accumulated a total of 71 557 cases (4.18‰) and 6 247 deaths.

Such differences cannot be explained by the median age of respective populations (43.4 versus 43.2 years old).

United Kingdom and Italy, (67.8 and 60.5 million people respectively) have population densities lower than Korea (272.9 and 205.8 inhab./Km^2 respectively). Both territories cover about 10° in latitude, but Britain is 10° further north. On the same date, 28th of August, United Kingdom had confirmed 338 083 cases and 41 589 deaths while Italy counted 269 214 cases and 35 483 deaths. When case numbers are averaged by respective population sizes, these European countries show up to a 13.1-fold increase relatively to South Korea. It is very unlikely that non-pharmaceutical measures implemented in the Asiatic country can explain such difference in cases, as well as in its reduced fatality rates. On the other hand, when comparing UK and Italy we found a 12% higher prevalence within this same period for Britain (4.98 versus 4.45‰) which is in accordance with its higher latitude. The fatality rates at the same reference date are comparable (12.3% versus 13.2% in Italy), but this is explained by a significant older population in Italy (average age 47.9 versus 40.8 in Britain).

As inferred from Table 1, which compares numbers in Asiatic countries with median latitudes below 40°N, lower prevalence and fatality ratios are also verified in Japan relative to Italy, despite its higher median age population and density. Latitude is the factor determining such differences also explaining why the other four countries in the Indochina peninsula, were not severely hit by the disease.

The fatality ratio was significant in Vietnam, possibly due to an uneven territorial development compared to South Korea and Japan or failure in detecting earlier positive cases. Some countries as New

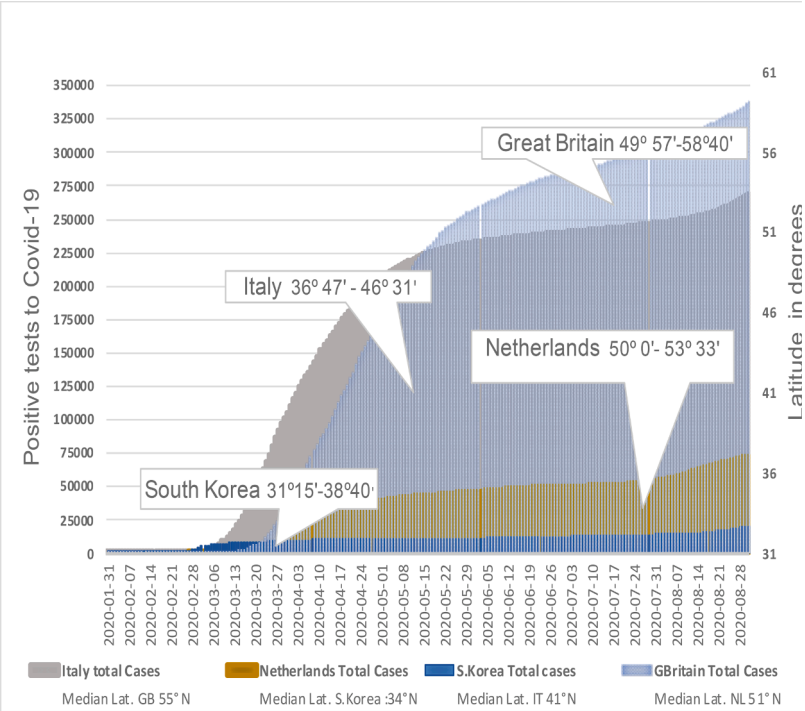

Fig. 1. Comparison of cumulative numbers of diagnosed Covid-19 cases in four countries within latitudes 30°–60°N on August 28, 2020. Great Britain and Italy, at higher latitudes have much more cases than South Korea while Netherlands with similar population density as S. Korea and one third of its population, has 3 times more cases.

Table 1
Comparison of cumulative number of Covid-19 cases and deaths in latitude frames of 8.5°N – 40° N in Asia[12].

Latitude	Location	Date	Total cases	Total deaths	Population	Population density	Median age	Period prevalence (‰)	Fatalities /case (%)
45°N-31.5°N	Japan	2020–08–28	66 499	1251	126 476 458	347.778	48.2	0.526	1.88
38°N-34.5°N	S. Korea	2020–08–28	19 400	321	51 269 183	527.967	43.4	0.378	1.65
22°N-14°N	Laos	2020–08–28	22	0	7 275 556	29.715	24.4	0.003	0
19.5°N-5.5°N	Thailand	2020–08–28	3410	58	69 799 978	135.132	40.1	0.049	1.70
14.5°N-10.5°N	Cambodia	2020–08–28	273	0	16 718 971	90.672	25.6	0.016	0
23.3°N-8.5°N	Vietnam	2020–08–28	1038	30	97 338 583	308.127	32.6	0.011	2.89

Zealand (lat. 41°S, averaged) found their latitude handicap compensated simultaneously by insularity and low-density population (4.8 million of inhabitants, 18.02 inhab./km^2). Thus, by the end of 2020 it counted just a total of 25 fatalities and 2162 reported cases (0.44‰) similar to those of countries like South Korea and Japan.

Across the African continent, progression of the disease was slow and the overall fatality ratio was significantly lower than in European countries as revealed by a study covering 55 African Union (AU) Member States [14], comparing the respective pandemic situation at December 31, 2020. The proportion of cumulative cases and deaths varied across the five geographical AU regions: 43% of cases and 46% of deaths in the southern region, 12% of cases and 9% of deaths in the eastern region, 34% of cases and 37% of deaths in the northern region, 3% of cases and 2% of deaths in the Central region, and 9% of cases and 5% of deaths in the western region. These numbers also reflect the impact of latitude across this continent as the diagnosed cases and

Table 2
Total cases of Covid-19 and deaths in equatorial countries as October 25, 2020[12].

Latitude	Continent	Country	Total Cases	Total deaths	Population	Population density	Prevalence‰	Fatalities/case%	Median age
10°S-0–5°N	Asia	Indonesia	389 712	13 299	273 523621	145.73	1.42	3.41	29.3
5°S-0–4°N	Africa	Congo	5253	92	5 518 092	15.40	0.95	1.75	19
4°S-0–4°N	Africa	Kenya	49 721	902	53 771 300	87.32	0.92	1.81	20
4°S-0–1°N	South America	Ecuador	161 635	12 553	17 643 060	66.94	9.16	7.77	28.1
4°S-0–2°N	Africa	Gabon	8919	54	2 225 728	7.859	4.01	0.61	23.1
0°–1.9°N	Africa	São Tomé & Principe	940	15	219 161	212.84	4.29	1.60	18.7
1°–1.7°N	Asia	Singapore	57 970	28	5 850 343	7915.73	9.91	0.05	42.4
1°S-0- 4°N	Africa	Uganda	11 443	101	45 741 000	213.76	0.25	0.88	16.4
4°N	Asia	Brunei	148	3	437 483	81.35	0.34	2.03	32.4
1°N-7°N	Asia	Malaysia	26 565	229	32 365 998	96.25	0.82	0.86	29.9

fatalities ratios are higher in regions nearby parallel 30° N and 30° S, with South Africa emerging as the worst affected (38.3% of a total of 2 763 421 cases).

Table 2 compares countries that are crossed by equator and refers to cumulated data as the 25th of October 2020. In equatorial regions, the consistency in decreasing numbers of infections is disturbed by particularities of some countries, although the fatalities per case remain low with exception of Ecuador.

This last country registered the highest number of cases (161 635) while deaths (12 553), were only slightly surpassed by Indonesia (13 299), a much larger and over 15 times more populated insular territory. The particularity of Ecuador lays on the geographic characteristics of its territory longitudinally crossed by the northern cordilleras of Andes, mountains with high peaks but populated, and where exists a colder weather contrasting with its Pacific coast which receives cool and warm currents. The much lower temperatures felt in the very high and much populated mountains, outweigh the UV radiation protecting effect expected of both higher altitude and lower latitude, facilitating the infections and aggravating their outcome. As for Singapore, the number of infections is significant, possibly higher, due to the extremely high population density, but there is no parallel in the fatality rate, which is the lowest despite the highest median age of the population.

When comparing, in Table 3, prevalence ratios in countries at higher average latitudes which are less populated territories, it may be concluded that population density has an effect but does not overweigh the effect of increasing latitude which is thus a major determining factor for higher infections rates and fatalities.

While we associate increasing latitude of countries with worsen pandemic ratios, Sajadi, M. M. and al (2020) [15], looking for seasonal patterns of Sars-CoV-2, and choosing a reference date in March 2020, compared 50 cities with negligible to significant spread of Sars-Cov-2. They concluded that 8 cities with substantial spread of the disease were located within the latitude corridor 30°−50°N, and those where deaths occurred, reached similar mean temperatures ranging from 2 to 10 °C for a period of 1 month or longer, and had low specific and absolute humidity. Cities as Moscow (56.0°N) and in the southeast of China as Bangkok (13.7°N) and Hanoi (21.2°N) had no deaths and few cases at the same reference date. They associated this to the pattern of survival of the respiratory coronavirus found in laboratory (4 °C and 20–80% relative humidity, RH) and pointed out to the risk of prolonged mean temperatures of 5–11° in new outbreaks associated with a RH range of 44%−84%. Another study [16], concerning approximately the same months from December through February, found some inconsistency in the association of these two variables in cities and provinces of China, but confirmed that median temperatures of 5 – 8° were favorable and that change in temperature had a more drastic effect in infections than the RH change beyond the range 67–86%.

These studies do not report the UV values in the cities considered, and were published before the 2nd wave, in the fall, when average temperatures are higher. An earlier letter [17] dismissed association with temperature or UV radiation, in Chinese cities both inside and outside Hubei. An opposite conclusion was drawn by a later study [18] with large cities in the US, confirming the effect of these factors in Covid-19 prevalence. These conclusions may not be contradictory if considered the different season of the initial pandemic outbreaks. Both studies follow a different design of that used in the study reported below.

3.2. Sars-Cov-2 daily incidence and fatalities correlations with UV of solar radiation

Low temperature considerations cannot explain why numbers of Covid-19 diagnosed cases and deaths in northern Europe and America exceeded largely those cumulated in equivalent populated areas in the Asiatic continent. In addition, the initial spread in those regions occurred just before or by the spring onset, when averages temperatures were already above 10°C.

In order to investigate how variation of solar UV light component impacted on the diagnosed Covid-19 cases and deaths, we choose two countries, Austria and Portugal and the ultraviolet indexes (UVIs) of respective capitals, Vienna (long. 16°22′, lat. 48°12′N) and Lisbon (long.−9° 10′, lat. 38° 42′ N), as both cities are considered representative of each country's latitude. Austria's frontiers fall within 46.5° and 48.75°N, approximately, and those of continental Portugal lay between 37°.75 and 42°.7°N. The two nations are similar with respect to surface and population (density 106.8 and 112.4 inhab./m^2, respectively). Excluding its Atlantic islands, Portugal's latitude difference at northern and southern borders is roughly 5°, justifying that daily UVI may differ between extremes as much as one unit or more. In Austria, such difference is narrower (2.3°) but, inversely, it spreads in longitude roughly 8°.

The results of both studies are reported in Fig. 2 (a – d) and 3(a and b). New daily cases tested positive to Covid-19 reported at national level in Austria were plotted along with daily UVI (clear sky) for the city of Vienne (the values extracted in included in tables S2a and 2b in Suppl. mat. 2).

The right arm side of the peak of Fig. 2c can fit the equation:

$$Y = 10\,188x^{-2.072}, R^2 = 0.9084 \quad (1)$$

where x is the UVI and Y the number of infections.

A clearer inversed power trend line was obtained corresponding to the equation:

$$Y = 11\,135x^{-2.122}, R^2 = 0.9572 \quad (2)$$

where x is the UVI and Y the number of infections, valid through the weeks starting July,18 and ending November, 20.

A similar regression analysis resulted for weekly averaged deaths, following within 6 weeks. The equation generated for deaths was:

$$Y = 64.681x^{-2.181}\, R^2 = 0.9620. \quad (3)$$

Table 4 summarizes the results of this study and respective square root mean errors and absolute mean error.

Portugal's first case of Covid-19 was detected on the 1st of March, later than in all European countries.

Fig. 3a covers the start of the pandemic crisis up to the end of 2020 and represents the evolution of new infections and deaths along with the

Table 3
Cases of Covid-19 and deaths in higher latitudes countries as of October 25, 2020[12].

Latitude (Average)	Continent	Country	Total cases	Total deaths	Population	Population density	Prevalence‰	Fatalites/cases%	Median age
60°N	North America	Canada	218 874	9995	37 742 157	4.037	5.80	4.57	41.4
60°N	Asia	Russia	1 503 652	25 875	145 934 460	8.823	10.30	1.72	39.6
61.25°N	Europe	Finland	14 848	353	5 540 718	18.136	2.68	2.38	42.8
62°N	Europe	Norway	17 909	279	5 421 242	14.462	3.30	1.56	39.7
62°N	Europe	Sweden	110 594	5941	10 099 270	24.718	10.95	5.37	41
62°N	Europe	Iceland	4448	11	341 250	3.404	13.03	0.25	37.3

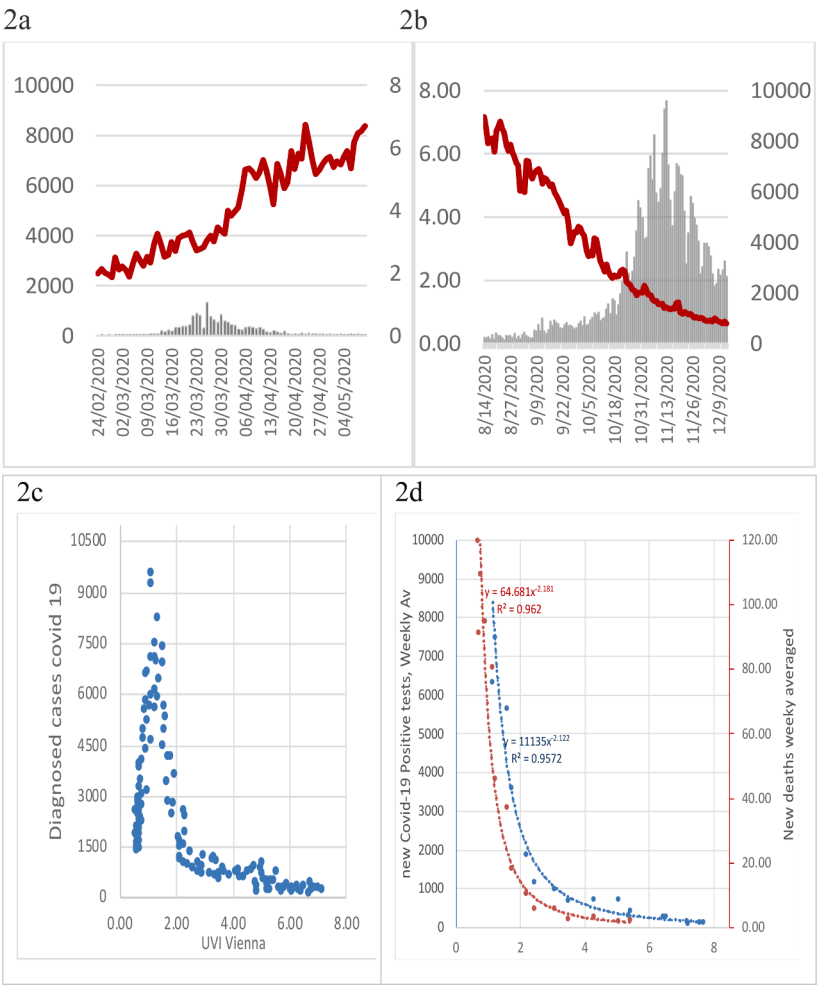

Fig. 2. Fig. 2a includes the first cases up to the end of the 1st wave in May, while Fig. 2b represents the evolution between mid-August and mid-December which includes the 2nd wave. The Fig. 2b, suggested a negative correlation between the steady increase of new diagnosed Sars-CoV-2 infections starting by the end of summer and the descendant trajectory of ultraviolet indexes (line above) from maximum values. This possibility was thus confirmed by the regression analysis of the two variables in this same period, resulting in the point scattered graphic represented in Fig. 2c. The correlation delivers a negative exponential progression of infections reaching a maximum, as the ultraviolet index approach 1 and regressing after that. The correlation is valid in the course of 4 months. Fig. 2d represents the same regression analysis, using the weekly averaged values, in order to offset inconsistencies arising in the reporting of new detected Covid-19 infections.

daily trajectory of the Lisbon UVI (upper line), with both variables weekly averaged.

Fig. 3b exhibits the regression analysis of new Covid-19 cases and deaths (weekly averaged) covering the period of the second pandemic wave.

A slightly better correlation was found for this second study. The curves obtained for Portugal fit a negative exponential trend described by equations:

$$Y = 15723e^{-0.485x},\ R^2 = 0.9755 \quad (4)$$

and

$$Y = 205.24e^{-0.579x},\ R^2 = 0.9765 \quad (5)$$

respectively for new infections and fatalities, where Y is the number of infections and x the UVI. The first equation relates values from the week starting on July, 25 up to November, 27 and the second, the fatalities occurring in the period of August, 29 ending January 1st, 2021. Deaths numbers predicted with this equation match well those registered. The results with the respective Root Mean Square Error (RMSE) and Mean Average Error (MAE) are summarized in Table 5, configuring satisfactory proximity between registered new positive cases and the model predicted values. It was also found, that if a delay of one week was applied, making new infections correspond to the index registered one week later, the equations describing infections would have the same trend and their R^2 was improved, $Y = 7243.9x^{-1.97}$, $R^2 = 0.9604$ (6) for Austria and $Y = 42187x^{-2.43}$, $R^2 = 0.98$ (7) for Portugal. The reverse movement, which made the registered infections, corresponds to the previous week's average indexes delivered weaker correlations. One explanation may be a weekly excess of false positive tests reported.

The Tables 4 and 5 correspond to the initial analyses, since this is the average for the two extreme situations (no anticipation or delay). Both studies produced comparable results, but R^2, RSME and MAE were better for Portugal. Explanation for this small difference might be the intensity of test screening but, more likely, the absence of cloud corrections in the ultraviolet indexes in the Austria study. The intensity of testing close to the 2nd wave peak, was lower in Austria (Table 6). Considering the averaged infections numbers and the week in which the peak occurred, Austria and Portugal tests outnumbered diagnosed cases by a factor of 4.3 (30 245/7464) and 6.3 (40 419/6386) respectively. A simulation, in the Austria study, with a 5% increase in the positive cases in the week of the peak, and the one preceding it, resulted in a slight lower R^2 and higher errors deviations (RMSE = 717.20, MAE = 358.31). Thus, a difference in volume of testing does not seem to explain the difference of results. The absence of UVI correction is favored.

UV indexes obtained from the Temis v2.0 UV index file, calculated for clear sky condition, may have to be modified by the presence of clouds. The application of the right coefficient correcting the clear sky index of a day requires ponderation, because the type of clouds may not disturb the sun light equally and, since the indexes are calculated around a specific time (local noon hour), it may not be necessary to apply a correction factor, if at this time, the sky is clear. Similarly, corrections are necessary in places at higher altitude. In the Portugal study, UVIs were corrected for clouds in the days associated with storms or heavy cloudy sky for long periods of the day (in Table 5 those weeks show indexes in italic). We also repeated the regression analysis after affecting

Table 4
Austria 2nd wave and regression analysis using weekly average (ave.) national infections and deaths[12] with Vienna UVI (July – November 2020).

Weeks	UVI (weekly average) (Vienna)[13]	New tested + (weekly ave.)[NT]	Forecast new tested + [NT]' $Y = 11135x^{-2.12}$	Δ [NT] -[NT]'	New deaths (weekly ave.)[ND]	New deaths forecast [ND]' $Y = 64.681x^{-2.187}$	Δ [ND]-ND]'
18 to **24/07/2020**	7.57	122	151.79	29.79	0.14	0.78	*RMSE=3.45*
25 to **31/7/2020**	7.69	126.71	146.81	−20.10	1.00	0.76	
01 to **07/8/2020**	7.22	97.14	167.83	−70.69	0.29	0.87	*MAE= 8.21*
08 to **14/8/2020**	7.19	148.71	169.32	−20.61	0.71	0.88	
15 to **21/8/2020**	6.53	268.29	207.70	60.58	0.71	1.08	−0.37
22 to **28/8/2020**	6.45	214.00	213.21	0.79	0.29	1.11	−0.82
29 to **4/9/2020**	5.36	302.00	315.79	−13.79	0.29	1.66	−1.37
5 to **11 /9/2020**	5.43	422.29	307.22	115.07	2.14	1.62	0.53
12 to **18/9/2020**	5.05	702.71	358.35	344.37	1.86	1.89	−0.03
19 to **25/09/2020**	4.29	720.43	506.54	213.89	3.29	2.70	0.59
26 to **2/10/2020**	3.49	696.29	784.90	−88.61	2.29	4.24	−1.81
3 to **9/10/2020**	3.06	973.43	1037.50	−64.07	5.57	5.64	−0.07
10 to **16/10/2020**	2.46	1171.29	1648.64	−477.35	5.86	9.08	−3.22
17 to **23/10/2020**	2.2	1861.14	2089.63	−228.49	10.29	11.59	−1.30
24 to **30/10/2020**	1.74	3594.43	3437.52	156.91	18.29	19.33	−1.04
31 to **6/11/2020**	1.6	5629.00	4107.22	1521.78	36.86	23.21	13.65
7 to **13/11/2020**	1.24	7464.14	7054.23	409.92	45.86	40.46	5.40
14 to **20/11/2020**	1.14	6303.29	8432.15	−2128.86	80.43	48.60	31.83
21to **27/11/2020**	0.92	5091.57			94.57	76.67	17.88
28 to **4/12/2020**	0.77	3750.43			109.29	113.41	−4.13
5 to **11/12/2020**	0.71	2762.29		*RMSE= 646.39*	91.14	134.68	−43.53
12 to **18/12/2020**	0.70	2618.86			119.71	139.87	−20.16
19 to **25/12/2020**	0.68	2020.29		*MAE=323.57*	93.71		
26/12 to **1/1/2021**	0.61	1979.43			68.29		

Austria's weekly average new cases tested positive (Nt) and new deaths by Covid-19 (Nd) (weekly averaged) versus predicted new cases (Nt') and new deaths (Nd') from the equations derived in regression analysis of Fig. 2d. UVI daily data for Vienna in table of Suppl. mat 2.

each UVI by the corresponding CMF (cloud modified factor obtained in the same data source [13]). This exercise resulted still in good correlations (R^2 = 0.9466 for diagnosed cases and 0.9582 for deaths), but inferior to those obtained with surgical corrections, as applied in some days, corresponding to higher impact of depressions and high instability conditions.

The weekly averaged maximums at the 2nd wave differed in Portugal and Austria for confirmed cases (6386 and 7464) and deaths (88 versus 119) (Tables 4 and 5). Considering the sum of the averaged cases tested positive through the same weeks divided by the population size, a higher prevalence was also found for Austria (3.12‰ versus 2.49‰). This difference cannot be due to population density, surface area or screening tests (all slightly higher in Portugal). We may rather find explanation in higher latitude of Austria as restrictions imposed in this period did not differ sufficiently in both countries. (After the 1st week in November a curfew between 20 h and 6 h in Austria, and from 22 h to 6 h in Portugal extended to week-ends after 13 h, but contrary to Austria, high schools and universities never closed).

Both studies satisfactorily explain the burst of Sars-CoV-2 infections into a dramatic second wave earlier than expected in the fall 2020, demonstrating that the decrease of solar ultraviolet irradiance, that parallels the descendant trajectory of UVI, is inversely related with the recrudescence of the pandemic virus infections, as no other environmental factor, changes globally and consistently through such a long period of the year.

Similar strong correlations could not be derived from the 1st spring wave. This is possibly related to the fact that UVIs have lower values than in the fall and are more impacted by small increases and decreases due to clouds, as noticed in index values of table S2-a (in Suppl. mat. 2) and in upper lines of Figs. 2a and 3a. In addition, the short duration of the wave prevents accumulation of sufficient volume of data needed for sharp correlations.

Examples of regression analyses with larger surface countries, Germany, France and Italy are shown in figures S2- 1a to 1f. (in Suppl. mat. 2)

In these and all other countries there was always a steady decrease of infections after the 1st wave as well as in the number of deaths, reaching their lowest levels, during late spring and summer, although cases persisted, frequently in clusters. Sars-Cov-2 maintains an infectious pattern beyond spring, contrary to Influenza and other respiratory virus, which have their highest activity in the Northern Hemisphere from late November to mid-February. Other beta coronavirus, as the MERS-CoV [19] of 2012, still remains active in some regions of the Arabian Peninsula, keeping its activity outside winter season. One explanation is possibly related to a reservoir species, the dromedary camel, capable of outstanding performances under extreme conditions in the desert, also possible vector of transmission to humans. In the case of Sars-Cov-2 reservoirs are likely human carriers.

As detailed further, some authors [20,21] justified, earlier in 2020, a potential sterilizing effect of solar radiation as summer approaches, which seemed in line with another study [22] which measured the decay period of infectivity of aerosolized samples of Sars-CoV-2, simulating solar light at different times of the year and with the virus suspended in different matrixes.

3.3. *Interference of temperature and humidity, as other relevant factors in pandemic recrudescence*

The evolution of coronavirus pandemic was followed beyond November in Austria and Portugal, revealing a divergent evolution (lighter entries, Tables 4 and 5). After the highest 2nd wave peak, and while the UVIs were still decreasing, the number of diagnosed daily cases started to regress in Austria, in a linear fashion (2c left side of the peak and Fig. 4a) for about 6 weeks, followed by a decrease in deaths, approximately 3 weeks later. In Portugal, new daily infections decreased until December, 25 (Fig. 4b), while fatalities met a stand-by in the last two weeks of 2020. Then, there was a sharp recrudescence of infections resulting into a new wave, with new maximums records of daily infections and deaths.

Several epidemiologists, politicians and the media in this country, blamed families for having abused the temporary relief of restrictions, afforded between the 23rd and 26th of December. Health authorities were accused of insufficient test screening covering two long weekends and the additional holidays that characterize celebrations of that month. Politicians, who had decided in favor of popular family relief measures, were also forced to assume their *mea culpas*.

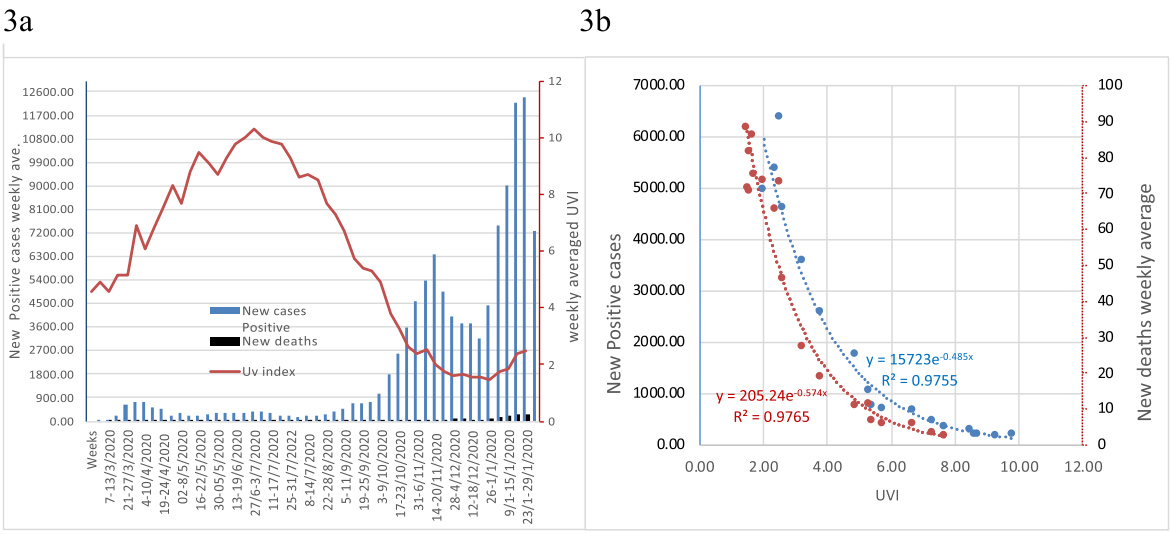

Fig. 3. Portugal's weekly averaged positive tests, to Covid-19 versus weekly average UV Index (Lisbon), 3a: Plot of the progression of national daily infections and deaths (weekly averaged) and UVI records from the end of February 2020 to end of January 2021. 3b: Reverse exponential correlation of UVI and Covid-19 infections from July 27 to November 20, 2020 (blue) and deaths (red) between Sept, 9 and Jan. 1st 2021.

However, the reality showed that all countries in the west end of Europe– Ireland, United Kingdom, Portugal and Spain– were hit sharply by an intense 3rd wave, within a couple of weeks difference, while eastern European countries saw daily cases numbers regressing after the 2nd wave, up to a stabilization.

The common event among those countries was an episode of intense cold. Portuguese territory, was affected in an unusual way between December, 26 and January, 13, 2021 [23]. During those days, 55% to 100% of the weather forecast stations registered minimal temperatures of 5 °C or lower and the air mean temperature of that period was 3 to 8 °C. This temperature range is in line with studies cited in Section 3.1 [15, 16], which concluded that the severity of Coronavirus 2020 outbreaks, was linked to temperatures as low as 5–8 °C or 2–10 °C, associated with medium to high relative humidity. Other authors [24] considered a wider optimal temperature of 5–15 °C, verified in about 60% of the several countries and regions studied, with a frequent peak at 11°, which would have caused the Sars-Cov-2's spreading, after the outbreak in China, into northern latitudes zones where such range of temperatures were in line with the season.

A cold snap had previously affected Ireland from beginning of December 2020. According to the Irish Meteorological Service, there was a cold polar maritime airmass that swept the country [25] which brought overnight and day-time temperature maximums of one figure and this was again the case in the last week of December, partially due to the storm Bella, also causing rain and hail. This storm also affected part of the British territory causing rain floods and overnight temperatures minimums and increase of snow and frost [26] up to the 1st week in January. In one month, the positive cases of Covid-19 in Ireland raise from 200 in earlier December, to a peak of 8221 by January, 8.

A few days later, exceptional cold weather reached Spain, due to the storm named Filomena. Madrid, the capital, was found immersed in a massive snow fall, not seen in the last 20 years and with temperatures as low as −10 °C, not felt over a century. These effects, lasted up to mid-January. As in Ireland and Portugal, there was an increase in Covid-19 cases and deaths. As shown in Fig. 5, daily positive tests peaked in Spain and in Portugal around the same weeks, delayed by two weeks from maximums registered in Ireland and United Kingdom.

The storm Filomena also reached Madeira, an autonomous region located at SW of Portugal at latitude 33°N, particularly between 6 and 8 of January 2021. This 780 Km^2 archipelago, was spared in the 1st Covid-19 wave and as December 23 it totalized only 11 deaths and 1343 cases. By January 26, daily numbers hit 160 infections while accumulated cases rose to 4661. About 3 weeks later, deaths had risen to 62 [27] representing a 5.4-fold increase in the islands, compared to 2.4 in the mainland and 2.83 in the Lisbon region. Although some media linked this outbreak to the British variant B.1.1.7 [28], the fact is that the 18 imported and detected cases at arrival in Madeira on the 27th of December had been isolated as procedures then adopted. The variant represented only a residual number of cases to justify the explosion of numbers, and thus cold or humidity felt in these islands is a more plausible explanation.

The recrudescence of Covid-19 in these western countries into an intense 3rd wave fits better the successive events of unusual cold and is independent of the stagnant UVIs which, as plotted in Fig. 5, are at their annual lowest. Very low temperatures may favor increased concentration of particulate matter and airborne particles above the ground level, favoring scattering and decreasing the perceived UV radiation.

When in the winter the UVI indexes reach their minimums, correlations with new daily infections cease. As seen in the months of July and August of 2020, most European countries' numbers tended to stabilize, oscillating at minimum levels. This also makes difficult any clear correlation of infections with Summer high temperatures in dry climates. Analyzing the number of cases reported in Lisbon district, between May 3rd and August 31st, no particular scattering pattern allowed a correlation with the daily median temperatures recorded between 11 and 28 °C (Suppl. mat. 2, figure S2–2).

High temperatures in combination with humidity seem to have an impact, as suggest the slight aggravation in cases and fatalities reported in some countries where the summer is humid. In Japan and South Korea, there are high relative humidity ratios in mid-summer. Plots in Fig. 6, comparing pandemic progression South Korea and Japan, show these mid-summer waves when UV indexes (upper lines) are near extreme highs. While with some significance, at least in Japan, where 73 deaths were registered between the 9th and 19th September 2020 [12], eventually corresponding to infections occurring in the July wave, the mid-summer waves were irrelevant in the countries of Indochina Peninsula (Fig. 7).

As reported in Table 1, Thailand, Vietnam, Laos and Cambodia, all on this peninsula, registered a reduced number of infections and deaths. This is in accordance with their lower latitudes, between 23.39°N (north of Vietnam) and 5.37°N (southern point of Thailand) and the consequent higher UV indexes, all year-round between 8 and 15 unities (upper line in Fig. 7). The pandemic wave in the fall did not have significance in these countries as they had in South Korea and Japan where UVIs have a

Table 5
Portugal's 2nd wave and regression analysis using weekly average national infections and deaths[12] versus UVI.

Weeks	New tested + (ave)*Tn]*	UVI Lisbon [13] weekly (ave.)	Forecast new tested + *[Tn]' y* = $15723e^{-0.485x}$	*Δ [Tn-Tn]'*	New deaths (ave)[ND]	New deaths forecast *y* = $205.24e^{-0.574x}$	*Δ [ND]-ND]'*
25 to **31/7/2020**	193.57	9.80	135.62	57.95	3.3		*RMSE=1.94*
01 to **07/08/2020**	175.29	9.30	172.84	2.44	1.6		
08 to **14//08/2020**	205.43	8.60	242.71	−37.29	3.7		*MAE=5.37*
15 to **21/8/2020**	210.00	8.70	231.22	−21.22	2.7		
22 to **28/8/2020**	285.14	8.50	254.78	30.37	3.3		
29 to**4/9/2020**	356.43	7.70	375.55	−19.12	2.6	2.5	0.1
5 to **11 /09/2020**	481.14	7.30	455.95	25.19	3.4	3.1	0.3
12 to **18/09/2020**	673.57	6.70	609.95	63.62	5.7	4.4	1.3
19 to **25/09/2020**	702.00	*5.72*	981.11	−279.11	6	7.7	−1.7
26 to **2/10/2020**	758.29	5.40	1145.83	−387.54	6.7	9.2	−2.5
3 to**9/10/2020**	1046.71	5.30	1202.77	−156.05	11.3	9.8	1.5
10 to **16/10/2020**	1768.71	4.90	1460.28	308.44	11.1	12.3	−1.2
17 to **23/10/2020**	2579.14	3.80	2489.61	89.53	18.7	23.2	−4.5
24 to **30/10/2020**	3595.71	3.24	3259.06	336.65	27.4	31.9	−4.5
31 to **6/11/2020**	4608.71	*2.63*	4391.08	217.63	46.3	45.4	0.9
7 to **13/11/2020**	5389.43	*2.39*	4933.14	456.29	65.43	52.1	13.4
14 to **20/11/2020**	6386.29	2.53	4609.30	1776.99	73.1	48.0	25.1
21to **27/11/2020**	4962.29	2.00	5960.33	−998.04	73.4	65.1	8.3
28 to **4/12/2020**	3990.57	1.73	6794.24		75.3	76.0	−0.7
5 to **11/12/2020**	3722.86	*1.59*		*RMSE=521.19*	81.4	82.4	−1.0
12 to **18/12/2020**	3726.71	1.67			86.3	78.7	7.6
19 to **25/12/2020**	3172.71	1.54		MAE= 292.42	71.6	84.8	−13.2
26/12 to **1/1/2021**	4410.57	1.55			70.6	8.3	−13.7
2/1 to **8/1/2021**	7473.86	1.46			88.30	88.8	−0.5

Positive cases of Covid-19 infections and deaths versus forecast numbers from the equations derived in regression analysis of Fig. 3b. UVIs in Italic mean that correction for clouds was applied in some days of that week by formula UVI = UVI_0 x CMF x (1 + 0.08 x ΔH) [8] where UVI_0 is the clear sky index. CMF is cloud modifying factor and ΔH is Height change, which is 0 in this case. CMF are from the Themis UV index overpass file [13] and are provided by MSG (Metaset Second Generation). Daily UVIs are listed in table S2b in Suppl. mat. 2.

Table 6
Tests performed versus cases detected, weekly averaged, at the 2nd wave peak[12] in Portugal and Austria.

Weeks in 2020	Infections (PT) (Ave.)	New tests (PT)(Ave.)	Infections (AT) (Ave.)	New tests (AT) (Ave.)	Tests x 10^6 /10 167 923 PT	Tests x 10^6 /9 043 072 (AT)
31/10–6/11	4608.71	36,068.71	5629.00	27,431.71	3547.30	3033.45
7/11 –13/11	5389.43	38,225.57	7464.14	30,245.43	3759.43	3344.60
14/11–20/11	6386.29	40,419.43	6303.29	30,437.57	3975.19	3365.84
21/11–7/11	4962.29	39,860.88	5091.57	28,580.86	3920.26	3160.53
28/11- 4/12	3990.57	32,811.29	3750.43	29,923.29	3226.94	3308.97

wider amplitude starting near 2 in Seoul in winter and rising to at least 12 units in the summer in Tokyo. Such variations enable correlations, as illustrated for South Korea and Japan (figures S2–3 and S2–4 in Suppl. mat. 2) at different periods of the year, more relevant in the fall, although wave amplitudes in both countries were lower than in northern European countries.

4. Discussion

This work highlights the role of UV sunlight radiation in shaping Sars-Cov-2 pandemic incidence from low to high latitudes. We provided illustration of strong quantitative correlations between the ultraviolet (UV) indexes, representing a territory and the detected cases or deaths reported within its borders. Besides the geographically delimitation of the territory, good correlations and the respective potential forecast value, rely on a robust screening of infected persons, not reduced on week-ends or holidays.

As observed after 1st wave peaks in the spring, infection rates and deaths regressed in all European countries in the latitudes of 37–60°N, contrary to Korea and Japan where a smaller summer wave was registered.

The modulation of the virus sensitivity across the globe possibly occurs through the UV solar components of UVB (280 to 320 nm), and UVA (320 to 410 nm), since these wavelengths reach the earth, although UVB also suffers partial absorption by the ozone layer and other propagation events. The sterilization power of solar UV radiation was estimated possible by some authors [20,21,29] at different latitudes in US and Europe, including Vienna and Lisbon, [21] where daily solar irradiance would reach the fluence thresholds estimated for viral RNA-damage in the UVB region. However, contrary to what was predicted and mostly observed with the Influenza A type virus [29], extended daily periods of solar exposition, in the spring and summer months were not enough to inactivate Sars-CoV-2 in those latitudes. The virus or pieces of its RNA persisted in carriers, accusing positivity in screening tests, but causing a more favorable outcome of the disease during all summer.

Most adverse biological effects related to sun exposure, from sunburns and photo-aging to DNA damage into different skin cancers, have been for long associated with wave bands in the region of UVB and UVA. As reviewed over the past decades [30,31], these effects are dependent on personal ultraviolet exposition and favored in identified risk groups [32]. UVA and UVB [33] may induce different type of immunosuppression pathways [34] reflecting their distinct penetrating powers, and different skin or eye chromophores.

An action spectrum, particularly strong with maximums at 300 nm [35] and at 370 nm [36], was found for an UV induced immunosuppression effect, interfering with innate and adaptive responses face to an antigen.

This effect was first discovered almost 50 years ago [37] in experiments with murine skin tumors. Its manifestation required a previous UV irradiation of skin before presentation to a specific antigen, allergen, virus or bacteria and fungus. Upon presentation of that antigen, an

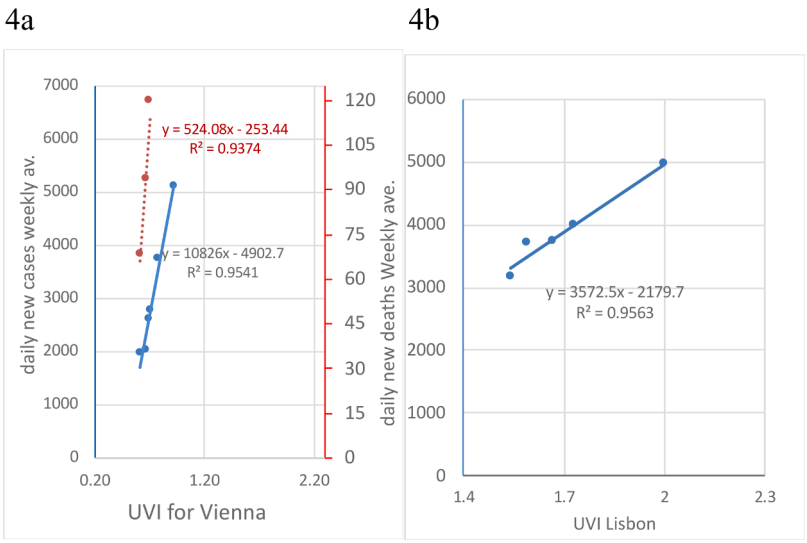

Fig. 4. Regression of new daily cases and UVIs after 2nd waves in Austria and Portugal. Fig. 4a: 2nd wave linear decrease of infections (blue) and deaths (red) in Austria (Nov. 20– Jan. 1st). Fig 4b: shorter decrease of cases in Portugal not followed by deaths (Nov. 20 – Dec 25).

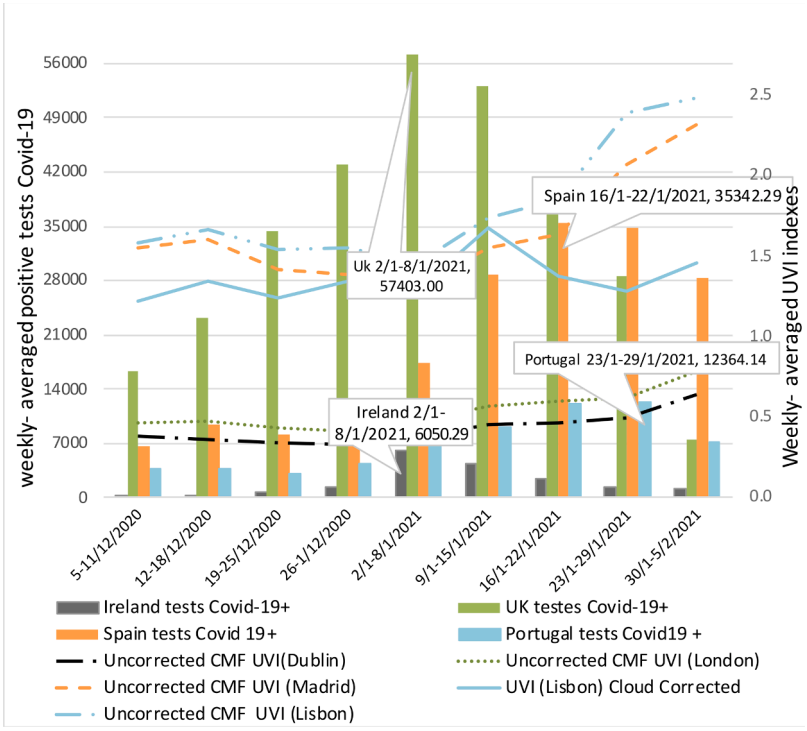

Fig. 5. 3rd (winter) wave of the four western European countries: Ireland, Portugal, Spain and UK. National weekly averaged diagnosed cases increase, while UVIs (Dublin, Lisbon, Madrid and London) stagnated at lower levels. Lisbon UVIs are shown uncorrected and corrected (line in full) were corrected by the CMF factor except for the week of 9–15 January. The other UVIs were left uncorrected.

immunity system previously exposed to that irradiation, fails to trigger the cascade events ending in local and systemic changes in the immune mediators, resulting in a possible increased susceptibility to infection and reinfection. As experiences with humans are unethical, progress in this field is achieved by extrapolation with animal infection models, but there are examples of infection resistance altered in humans by ultraviolet radiation such as HSV (Herpes simplex Virus), HVP (Human papillomavirus), fungus and non-skin associated infections [38].

As correlations with UVI indexes show, the Sars-Cov-2 incidence is related to solar UV light and linked to evident risk groups, suggesting that the person-to-person virus transmission pattern co-exists with UV-induced immunosuppression response modulating humans encounter with this viral antigen.

The fact that UVB is mostly filtered through glass windows, whereas UVA is not, also explains different affected populations. Thus, is possible to link Covid-19 risk incidence to a family event in-doors as well as to outdoor workers, or to those whose recreative or professional activities expose them to substantial periods outside, in circumstances where viral charge is not expected to be high.

The mechanism of UV-induced immunosuppression is antigen specific. It arises following exposure to individual doses of solar UV radiation and subsequent encounter within a variable but relative short

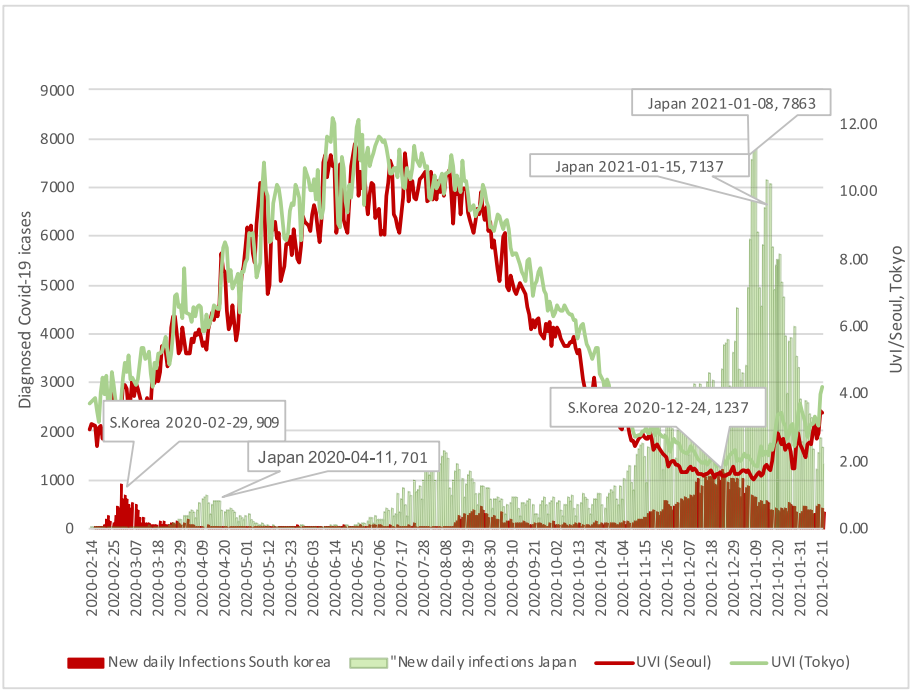

Fig. 6. Above: South Korea and Japan infection cases versus UVI (Seoul and Tokyo). Evolution of Covid-19 in these countries differs in 2020 of those in northern latitudes by a reduced number of infections and deaths and an increase of cases in mid-summer (summer wave).

delay with, in this case, Sars-CoV-2 antigenic units, or aerosolized virus released from undiagnosed or asymptomatic carriers. Such events can occur through spring to earlier fall, when populations are frequently exposed to UV sunlight radiation. This explains sustained infection in clusters which progress quicker as falls installs, since infectivity of the virus and transmission is simultaneously increasingly favored by decreasing UV. In between fall and spring waves, additional waves can arise when low temperature or higher temperature associated with humidity match optimal range of virus survival. In the winter, when UV radiation is at its lowest, and human susceptibility is high, the disease outcome is aggravated. In the summer is favorable.

The clear-sky UV indexes used are based on the erythema action spectra [9] integrating wavelengths in the UVB and UVA region but with a maximum at 300 nm. The biological action spectra of UV induced-immunosuppression have one of its maxima at 300 nm which may explain why it was possible to find correlation between values of these UV indexes and numbers of infections. These correlations, if associated with reliable and *consistent* test screening in a geographic

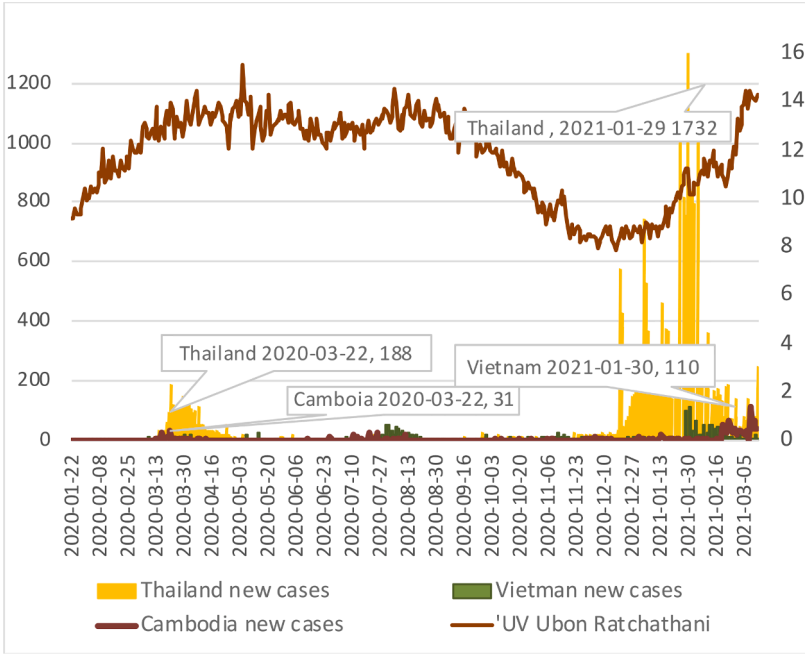

Fig. 7. Infections by Covid-19 in three countries in the Indochina peninsula. Thailand, Vietnam and Cambodia. UVI is from Ubon Ratchathani (long. 104.86°E and latitude 15.26°N), location approximately in the center of this peninsula showing very high indexes all year round. The larger surface country registers the highest incidence.

delimited region, could be turned into indispensable forecasting tools in latitudes of higher incidence, helping communities shaping preventive measures in different regions, provided they are adequately delimited. The examples provided with regression analyses of the two chosen countries (Austria and Portugal) confirmed the small quantitative differences of number of cases at the 2nd wave. Carried on into earlier 2021 the exercise also predicted a different pandemic evolution in the two countries.

After the fall wave, Portugal entered into a dramatically strong 3rd wave, but assisted afterwards to a rapid regression of number of cases and deaths not feeling any perceptible wave by March-April of 2021 (Fig. 8a). On contrary, in Austria, (Fig. 8b) after the subsequent sharp decrease following the 2nd wave, the numbers of new cases remained oscillating at sufficiently high levels, rising later in a still significant spring 3rd wave. In this wave the daily maximums reached 3 895 infections and 42 deaths. A potential effect of vaccination numbers on such different outcomes is excluded as the relative excess in Portugal is not significant (631 501 versus 535 469 vaccinations in Austria as of the 1st of March) [12].

Much work still needs to be done to clarify current pandemic global spread as well as implications of a possible UVA/UVB mediated immunosuppression response in the clinical outcomes of the disease as well as on alternatives to prevent or fight pandemics, hopefully quicker and less expensively than by mass vaccination.

5. Conclusion

In this study we investigate quantitative correlations between pandemic coronavirus RT-PCR detected cases and ultraviolet indexes (UVI) at selected locations, explaining the role of UV-sunlight in the daily outcomes of Sars-Cov-2 infections and deaths.

While these correlations are applicable when UVIs trajectory is ascendant or descendant, they became more evident at the occurrence of the fall pandemic waves. As shown with the examples of Austria and Portugal, limited territorial areas are required for strong correlations. We also provide explanation for 3rd waves which emerged in winter 20/21 in western European countries, based on optimal ranges of temperature and humidity. Considering that increase of infections by Sars-Cov-2 are latitude dependent, and can be correlated with UVI-Erythema derived indexes in the UVB-UVA spectral region, we are tempted to conclude that the disease is caused, apart from the usual airborne and droplet viral transmission, by a sunlight-UV-induced immunosuppression response, with wavelengths maximums in the UVB and UVA region. This would explain cases of Covid-19 detected in unexpected groups working many hours outside (construction workers, agricultural laborers, outdoors athletes) and apparently non-related higher mortality associated in pandemic years. This finding has different consequences and should be further investigated. [39,40,41]

Supplementary material 1

Materials and methods

Raw data, (i.e. not smoothed by any kind of ratio regarding population), was collected from the database “our world in data” [12], and up-to-dated periodically to integrate eventual corrections by primary sources. The data extracted for countries addressed in this study consisted in numbers of daily positive cases, daily deaths and daily tests, population, population density and median age of population. The numbers of cases and deaths were compared with national health authority official daily bulletins of one of the countries [39] and were found identical. In Section 3.1 latitude versus disease analysis, “Prevalence ratios” in tables 1, 2 and 3 correspond to the quotient of the number of diagnosed cases over the population size expressed per thousand (‰). Fatality ratios are expressed percent (%) and correspond the quotient of number of deaths over the total of diagnosed cases. The

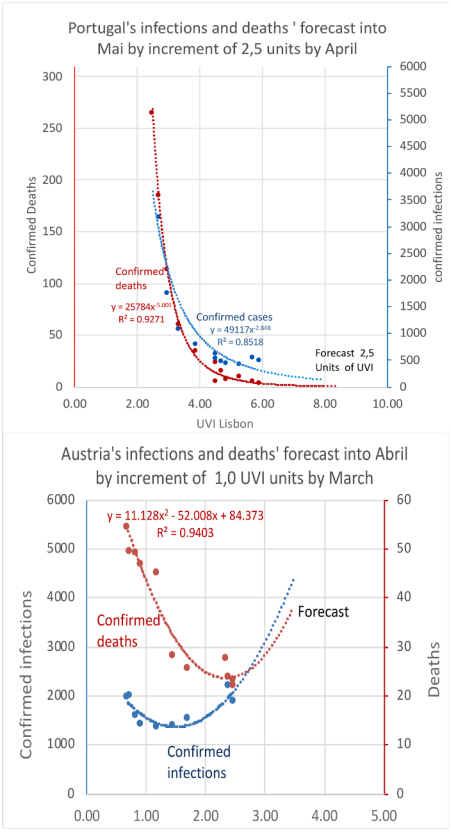

Fig. 8. Weekly averaged correlations after decrease of infections following 3rd wave in Portugal (8a) and after 2nd wave in Austria (8b) and respective forecasts. Full lines cover January 30 – Abril 23 (8a) and January 2nd – 5 March 21 (8b) While no wave was foreseen in Portugal with deaths approaching zero, in Austria an increment of 2,5 – 3,5 UVI units forecasts a value around 4000 cases as reached in the 3rd wave of this country.

ratio of total testes performed per total cases found (positive tests) was calculated at the reference date but not reported in tables and was 31.7 in Italy, 30.8 in UK, 16.3 in Netherlands, 94.7 in South Korea, 19.2 in Japan and 266.4 in Thailand, 940.6 in Vietnam, 650.3 in New Zealand, 49.3 in Canada, 38.5 in Russia.

The UV indexes source is the *Temis v2.0 UV index and UV dose overpass file* [13] of the Temis (Tropospheric Emission Monitoring Internet System) satellite database that monitors the ozone layer in the troposphere. This database resulted from joint efforts of an international consortium of different research groups who, back in 1996 [40], rendered accessible and standardized daily UV indexes for many point locations at different latitudes.

Regression analyses in Section 3.2: Choice of UIV locations: among the cities with UVI data available in the source data file were chosen those which filled the criteria of being highly populated and closer to the average latitude of the respective country/region. The values extracted from the satellite file are those of the 1st column of the 16-column grid, thus the clear sky index reported daily for Vienna (long. 16.35′° and lat. 4823°N) and for Lisbon (long.−9.15° lat. 38.77°N). The clear sky indexes were also collected for Berlin, Paris, Ispra, Seoul and Tokyo and used in the correlations illustrating the effect in larger European and Asian countries and placed in Supplement material 2. The table S2-*a* reproduces some of these UV indexes, while they are increasing, as at the occasion of the 1st wave (March up to mid-April of 2020), while table S2-*b* lists decreasing values after reaching maximums in the summer and up to the end of the 2nd wave. UV index derived for a sky without

clouds, can be reduced by a factor of 0.2 to 1 (no correction) depending on the type of clouds (high, medium and low) as can fog and rain by factors of 0.4 or 0.2[8]. The Cloud Modifying Factors (CMF) were obtained from the 15th column of the same Temis v2.0 UV index and UV dose overpass file and applied, in the case of the Portugal study, in days where the UV indexes forecasted in the national weather forecast institute homepage [41] for Lisbon had been reduced, mostly by particularly cloudy days. In the weeks containing such days the clear sky index is multiplied by the corresponding cloud modifying factor and that week average value is reported in Table 5 in Italic.

Data used to derive Eqs. (2) and (3) is the weekly UVI averaged values and weekly averaged diagnosed cases taken between July, 18 and November, 20 and UVIs and deaths, weekly averaged, between September, 5 and December, 18 table 4 referring to Austria). For Eqs (4) and ((5) the weeks considered are from July, 25 to November, 27 and August 29 to January 8, 2021 respectively (Table 5 referring to Portugal). From the XY point scattered chart option obtained in Microsoft Excel, Macintosh version, 16.16.27, 2018© for each pair of variables, was chosen the best trendline providing higher R^2 and the corresponding equation. Square root mean error (SRME) and Mean absolute error (MAE) were also derived from the function options. This same procedure was used to obtain graphics covering subsequent periods (November to December 2020 in Figs. 4a and January to April in Figs. 8a and 8b)

Study of other relevant factors in Section 3.3: The number of positive tests to Covid-19 was extracted from referenced source for Ireland, Portugal, Spain and United Kingdom and averaged for every week starting on the December 5 and ending on February 5, 2021. The UVIs collected from Dublin, Lisbon Madrid, London were weekly averaged in the corresponding week. The average latitude criterion for these locations were sought but was not so important as the study is not intended to derive a quantitative relationship between UVIs and cases detected in respective countries. For the Japan and South Korea study, daily infections and daily UVIs of Seoul and Tokyo were extracted between February 2020 and February 2021 and used directly in graphic assembly. In the Indochina peninsula infection data was from Thailand, Cambodia and Vietnam. The daily UVIs values were extracted from an averaged latitude location of the peninsula found in Ubon Ratchathani. The same Excel software referred above was used for the bidirectional graphics of these sections.

Latitudes are all approximate values and were obtained from the site of mapsofword.com or alternatively from Wikipedia.

7. Funding

This research did not receive any specific grant from funding agencies in the public, commercial, or not-for-profit sectors.

Declaration of Competing Interest

The author has no conflict of interests

Acknowledgements

The author is very grateful to Joana Baptista for our research discussions and technical advice on MS Excel© tools as well as to Nicole Darabian, Pilar Viegas, Odete and Carlos Nascimento for their assistance in the manuscript proof reading.

Supplementary materials

Supplementary material associated with this article can be found, in the online version, at doi:10.1016/j.jpap.2022.100108.

References

[1] Brian Beach, Karen Clay, Martin.H. Saavedra, "The 1918 Influenza Pandemic and Its Lessons for Covid-19". NBER Working Paper Series n° 27673, National Bureau of Economics, Cambridge, MA, 2020. ©..
[2] David M Mourns, Anthony S. Fauci, The 1918 influenza pandemic: insights for the 21st century, J. Infect. Dis. 7 (195) (2007) 1018–1028. Issue1 April.
[3] Peng Zhoul, Xing-Lou Yang, Xian-Guang Wang, et al., Pneumonia outbreak associated with a new coronavirus of probable bat origin, Nature (579) (2020) 270–275.
[4] World Health Organization Writing Group, "Nonpharmaceutical interventions for pandemic influenza international measures, Emerg. Infect. Dis. 12 (1) (2006) 81–87, 10.3201/eid1201.051370.
[5] Carcione, J.M., Santos. J.E., Bargain C., Ba J. "A simulation of a COVID-19 epidemic based on a deterministic SEIR model". Front public health. (2020) May 28, 8:230. https//doi.org 10.3389 /fpubh.2020.00230 . PMID: 32574303, PMCID: PMC7270399.
[6] Giacomo Cacciapaglia, Corentin Cot, Francesco Sannino, et al., Second wave Covid-19 pandemics in Europe: a temporal playbook, Nat. Sci. Rep. 10 (2020) 15514, https://doi.org/10.1038/s41598-020-72611-5.
[7] Alison L. Hill, The math behind epidemics, Phys. Today 73 (2020) 11, 28 10.1063/PT.3.4614.
[8] Karel Vanicek, Thomas Frei, Zenobia Litynska, Alois Schmalwieser, UV-Index for the public: a guide for publication and interpretation of solar UV index forecasts for the public prepared by the working group 4 of the cost-713 action "UVB forecasting, Brussels (1999).
[9] ISO CIE 18166: 1999 "Erythema reference action spectrum and standard erythema dose.
[10] Marc Alaart, Michiel van Wile, Paul Fortuin, Hennie Kelder, An empirical model to predict the UV Index based on zenith angles and total ozone, Meteorological. Appl. 11 (2004) 59–65, https://doi.org/10.10177/S1350482703001130. Doi.
[11] Aleksandr Ianevski, Eva Zusinaite, Nastassia Shtaida, et al., Low temperature and low UV indexes correlated with peaks of influenza virus activity in Northern Europe during 2010-2018", Viruses 11 (3) (2019) 207, 10.3390/v11030207.
[12] Roser, Max, Ritchie, Hannah, Ortiz-Ospina, Esteban, and Hasell, Joe (2020), "Coronavirus pandemic (COVID-19)". Published online at OurWorldInData.org. Retrieved from: 'https://ourworldindata.org/coronavirus' [Online Resource].
[13] Van Geffen, J., Van Weele, M., Allaart, M., and Van der A.R. (2017) TEMIS UV index and UV dose operational data products. Version 2. Dataset. Royal Netherlands Meteorological Institute (KNMI). doi.org/10.21944/temis-uv-oper-v2.
[14] Stephanie Salyer, Justin Maeda, Senga Sembuche, et al., The first and second waves of the Covid-19 pandemic in Africa: a cross-sectional study", Lancet (2021) https://doi.org/10.1016/S0140-6736(21)00632-2. Published Online March 24.
[15] Mohammad M. Sajadi, Vintzileos Habibzadeh, Parham, et al., Temperature humidity and latitude analysis to predict potential spread and seasonality of Coronavirus disease 2019 (Covid19), JAMA Netw. Open 3 (6) (2020) e2011834 doi:10.1001/jamanetworkopen.2020.11834: or http://dx.doi.org/10.2139/ssrn.3550308.
[16] Hongchao Qi, Shuang Xiao, Runye, Shi, Covid-19 Transmission in Mainland China is associated with temperature and humidity": a time series analysis, Sci. Total Environ 728 (2020), 138778, https://doi.org/10.1016/j.scitotenv.2020.138778 https://doi.org.
[17] Ye Yao, Jinhua Pan, Zhixi Liu, et al., No association of Covid-19 transmission with temperature or UV radiation in Chinese cities, Eur. Respir. J. 55 (2020), 2000517, DOI: 10 1183/13993003.00517-2000.
[18] Hisato Takagi, Toshiki Kuno, Yujiro Yokoyama, et al., The higher temperature and ultraviolet, the lower Covid-19 prevalence -meta-regression of data from large US cities" Am, J. Infect. Control 48 (10) (2020) 1281–1285. Oct.
[19] Alshukairi, Abeer N, Zheng, Jian, Zhao, Jingxian et al. "High prevalence of MERS-CoV infection in Camel workers in Saudi Arabia" mBio.asm.org (2018) Oct30. 9 (5) e01985-18. 10.1128/mbio.01985-18.
[20] Sagripanti, Jose-Louis, Lytle, C.David. "Estimated Inactivation of Coronavirus by solar radiation with special reference to Covid-19" "Photochem. Photobiol." (2020) 96: 731–737 DOI: 10.1111/php.13293.
[21] R.S. Carvalho, Fernanda, V. Henriques, Diamantino, Osvaldo Correia, W. Schmalwieser, Alois, "Potential of solar Radiation for inactivation of Coronaviridae family estimated from satellite data", Photochem. Photobiol. 97 (2021) 213–220, doi: 10.1111/php.13345.
[22] Michael Chuit, Shanna Ratnesar-Schumate, Jason Yolitz, et al., Airborne Sars-CoV-2 is rapidly inactivated by simulated sunlight, J. Infect. Dis. 222 (4) (2020) 564–571.
[23] Instituto do Mar e da Atmosfera, "Episódio de frio persistente de Dezembro a Janeiro 2021" (2021) version 2.2 up-to-date January, 14. (2021) Lisbon. https://www.ipma.pt/pt/media/noticias/documentos/2021/acompanhamento-jan-2021-atualizacao_dia13-vrs2.2.pdf Last accessed October 2021.
[24] Zhongwei Huang, Jainping Huang, Qianging Gu, et al., Optimal temperature zone for the dispersal for Covid-19, Sci. Total Environ 736 (2020), 139487. Sep 20.
[25] https://cli.fusio.net/cli/stormcenter/Bella.pdf.
[26] News, 2021, https://inews.co.uk/news/uk-weather-met-office-forecast-ice-cold-start-2021-815012.
[27] "Covid-19 Relatório de situação epidemiológica na RAM in 13.02.2121- "Covid-19 in regional secretary of health protection of Madeira" https://covidmadeira.pt/publicacao/covid-19-relatorio-de-situacao-epidemiologica-na-ram-em-13-02-2021/Last accessed October 2021.

[28] N.G. Davies, Sam Abbott, C. Barnard Rosanna, et al., Science "Estimated transmissibility and impact of Sars-Cov-2 linage B.1.1.1 in England, Science (2021), 10.1126/science abg 3055.
[29] Sagripanti, Jose Louis and Lytle, C.David "Inactivation of influenza virus by solar radiation" Photochem. Photobiol. (2007) 83: 1278–1282.
[30] May Norval, Gary M Halliday, The consequences of UV-induced immunosuppression for human health, Photochem. Photobiol. 87 (2011) 965–977.
[31] Jamie J. Bernard, Richard L. Gallo, Jean Krutmann, How ultraviolet radiation affects the immune system, Nat. Rev., Immunol. 19 (2019) 688–701, 10.1038/s41577-019-0185-9.
[32] Godar, Diane E. "UV doses worldwide" Photochem. Photobiol. (2005) 81: 736–749 10.1111/j.1751-1097.2005.tb01438.x.
[33] Terence S.C. Poon, Ross St.C Barnetson, G.M. Halliday, Sunlight-induced immunosuppression in humans is initially because of UVB, then UVA, followed by interactive effects, J. Invest. Dermatol. 125 (2005) 840–846.
[34] Rana Sabita, Scott Napier Byrne, Linda Joanne MacDonald, et al., Ultraviolet B suppresses immunity by inhibiting effector and memory cells, Am. J. Pathol. 172 (4) (2008) 993–1004, https://doi.org/10.2353/ajpath.2008.070517, doi:. Epub 2008 Feb 21.
[35] Y.J. Matthews, G.M. Halliday, T.A. Phan, D.L. Damian, A UVB wavelength dependency for local suppression of recall immunity in humans demonstrates a peak at 300 nm, J. Invest. Dermatol. 130 (2010) 1680–1684.
[36] D.L. Damian, Y.J. Matthews, T.A. Phan, G.M Halliday, An action spectrum for ultraviolet radiation-induced immunosuppression in humans, Br. J. Dermatol. 164 (3) (2011) 657–659.
[37] M.L. Kripke, Antigenicity of murine skin tumors induced by ultraviolet light, J. Natl. Cancer Inst. 53 (5) (1974) 1333–1336.
[38] Annemarie Sleijffers, Johan Garssen, Henk Van Loveren, Ultraviolet radiation to infectious diseases and vaccination responses, Methods 28 (2002) 111–121.
[39] https:/covid19. min-saude.pt/wp-content/uploads/2020/08/161 _DGS_boletim_20200810 or https://covid19.min-saude.pt/wp-content/uploads/2021/06/460_DGS_boletim_20210605.pdf (as an example), last accessed 06/ 2021.
[40] WMO. Report of the WMO-WHO meeting of experts on standardization of UV indices and their dissemination to the public (Les Diablerets. 21-24 July. 1997). GAW. Report No.127. Geneva. 1998.
[41] IPMA. https://www.ipma.pt/pt/otempo/prev.localidade.hora.